J|A|C|S
ARTICLES
Published on Web 03/16/2006

Molecular Tweezer and Clip in Aqueous Solution: Unexpected Self-Assembly, Powerful Host−Guest Complex Formation, Quantum Chemical ^{1}H NMR Shift Calculation

Frank-Gerrit Klärner,*[†] Björn Kahlert,[†] Anke Nellesen,[†] Jan Zienau,[‡] Christian Ochsenfeld,[‡] and Thomas Schrader[§]

Contribution from the Institut für Organische Chemie der Universität Duisburg-Essen, 45117 Essen, Germany, Institut für Physikalische Chemie und Theoretische Chemie der Universität Tübingen, 72076 Tübingen, Germany, and Fachbereich Chemie der Universität Marburg, 35032 Marburg, Germany

Received December 12, 2005; E-mail: frank.klaerner@uni-essen.de

Abstract: The newly prepared water-soluble naphthalene tweezer **2a** and anthracene clip **4a** (substituted both with lithium methanephosphonate groups in the central spacer unit) undergo an unexpected self-assembly in aqueous solution. The highly ordered intertwined structures of the self-assembled dimers $[\mathbf{2a}]_2$ and $[\mathbf{4a}]_2$ were elucidated by quantum chemical ^{1}H NMR shift calculations. **2a** and **4a** form extremely stable host−guest complexes with *N*-methylnicotinamide **8** in methanol and water as well. According to the thermodynamic parameters determined by ^{1}H NMR titration experiments at various temperatures the self-assembly of **2a** and **4a** and their strong binding to NMNA **8** observed in aqueous solution are enthalpy driven ($\Delta H \ll 0$); the enthalpic driving force is partially compensated by an unfavorable entropy ($T\Delta S < 0$). Self-assembly and the host−guest binding are therefore beautiful examples of the nonclassical hydrophobic effect.

Introduction

Efficient synthetic receptors with the capability for selective substrate binding in aqueous solution are important for the understanding of molecular recognition and self-assembly in chemical and biological systems.[1,2] Hydrophobic interactions are one of the crucial forces, which determine stability and structure of supramolecules in water.[3] Essential examples involve protein folding;[4,5] protein−ligand (e.g., enzyme−substrate) binding;[6,7] protein−protein association;[8−11] supramolecular complex formation by the interaction of nonpolar host and guest domains; the self-assembly of surfactants to micelles, bilayers, and other supramolecular structures; and the solubilization of nonpolar substances by surfactant aggregates.[12] Traditionally, hydrophobic interactions are predicted to increase steadily and incrementally as the surface area of the solute is enlarged with respect to the well-ordered water molecules in liquid phase. The release of water molecules into the solvent bulk during the aggregation of the solute leads to an increase in entropy (classical hydrophobic effect, entropy-driven).[3,13] Recent investigations of recognition processes, for example, of host−guest complex formations, enzyme substrate binding, or DNA intercalation by arenes, however, show that in these cases an enthalpic gain is the origin of hydrophobic interactions (nonclassical hydrophobic effect).[3,14−17] The smallest conceivable ordered supramolecular structure resulting from a self-assembly between nonpolar domains of molecules of the same kind is a dimer. Biological and synthetic examples include hemoglobin (each of the four subunits consists of an α,β-

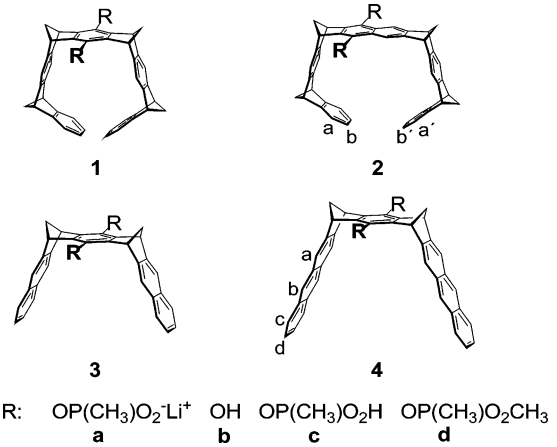

[†] Universität Duisburg-Essen.
[‡] Universität Tübingen.
[§] Universität Marburg.

(1) Lehn, J. M. *Supramolecular Chemistry. Concepts and Perspectives*; Wiley-VCH: Weinheim, 1995.
(2) Atwood, J. L. *Comprehensive and Supramolecular Chemistry*; Pergamon: Oxford, 1996.
(3) Meyer, E. A.; Castellano, R. K.; Diederich, F. *Angew. Chem., Int. Ed.* **2003**, *42*, 1210−1250.
(4) Dill, K. A. *Biochemistry* **1985**, *24*, 1501−1509.
(5) Alonso, D. O. V.; Dill, K. A. *Biochemistry* **1991**, *30*, 5974−5985.
(6) Houk, K. N.; Leach, A. G.; Kim, S. P.; Zhang, X. *Angew. Chem.* **2003**, *115*, 5020−5046.
(7) Landschulz, H. W.; Johnson, P. F.; McKnight, S. L. *Science* **1988**, *240*, 1759−1764.
(8) Stites, W. E. *Chem. Rev.* **1997**, *97*, 1233−1250.
(9) Jones, S.; Thornton, J. M. *Proc. Natl. Acad. Sci. U.S.A.* **1996**, *93*, 13−20.
(10) Bogan, A. A.; Thorn, K. S. *J. Mol. Biol.* **1998**, *280*, 1−9.
(11) Larsen, T. A.; Olson, A. J.; Goodsell, D. S. *Structure* **1998**, *6*, 421−427.
(12) Schneider, H.-J.; Yatsimirsky, A. *Principles and Methods in Supramolecular Chemistry*; Wiley-VCH: Weinheim, 2000.

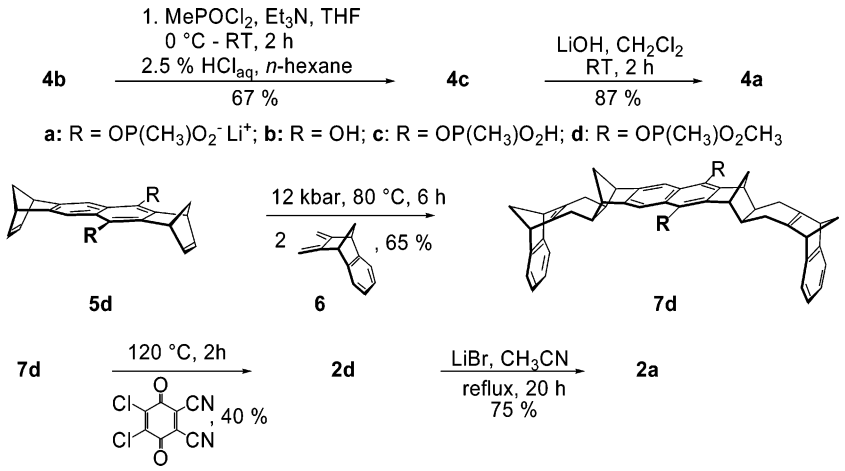

Figure 1. Synthesis of water-soluble clip **4a** and tweezer **2a**.

heterodimer)[18] molecular capsules[19−22] and the self-assembled dimers of methylene-bridged glycoluril derivatives.[23−25]

Recently, we have described the water-soluble benzene-spaced molecular tweezer **1a**[26] and the benzene-naphthalene-spaced molecular clip **3a**.[27,28] They are both monomeric species and bind biologically important molecules such as cofactors of enzymes and peptides in aqueous solution with remarkable efficiency and selectivity. By enlarging their respective π-faces we sought to improve and further modify their recognition abilities. Here, we report the synthesis of the water-soluble phosphonate substituted naphthalene-spaced tweezer **2a** and benzene-anthracene-spaced clip **4a** and their spontaneous self-assembly in aqueous solution leading to highly ordered intertwined structures. We were quite surprised that these new hosts form highly stable dimers in aqueous solution. This efficient dimerization, however, is overruled if *N*-methylnicotinamide iodide (NMNA) is added to an aqueous solution of **2a** or **4a**. An exceedingly strong binding of NMNA as guest molecule inside the host cavity is observed. The structures of both monomers **2a** and **4a** and their self-assembled dimers $[\mathbf{2a}]_2$ and $[\mathbf{4a}]_2$ were elucidated by quantum chemical ^{1}H NMR shift calculations. By experimental determination of the underlying thermodynamic parameters we were able to characterize the self-assembly and complexation processes as beautiful examples of the nonclassical hydrophobic effect.[3,14−17]

Results and Discussion

The anthracene clip **4a** could be prepared analogously to the naphthalene clip **3a**[27,28] starting from the hydroquinone **4b**.[29] The deprotonated form of **4b** was treated with methanephosphonic acid dichloride ($CH_3P(O)Cl_2$, $N(C_2H_5)_3$, THF), followed by hydrolysis of the remaining chloro substituents (2.5% HCl_{aq}, *n*-hexane). The resulting phosphonic acid **4c** (yield: 67%) was subsequently deprotonated with 2 mol equiv of LiOH leading to the desired lithium phosphonate clip **4a** which is soluble in water and methanol, as well (Figure 1).

For the synthesis of the tweezer **2a** we had to apply a different route since the naphthohydroquinone tweezer **2b** is highly sensitive to oxidation and could not be isolated to date. Therefore, hydroquinone bisdienophile **5b** (R = OH)[30] was converted to the corresponding methyl methanephosphonate **5d** by reaction with $CH_3P(O)Cl_2$ in the presence of triethylamine followed by methanolysis (yield: 30%). **5d** reacts with diene **6** in the fashion of repetitive Diels−Alder cycloadditions stereoselectively on the *exo* face of the bisdienophile and the *endo* face of the diene leading to the bisadduct **7d** having all four methylene bridges on the same side of the molecule. At atmospheric pressure and high temperature (1bar and 160 °C) only products of decomposition of either the cycloadduct or the starting materials are observed. An increase in pressure up to 12 kbar leads to the expected acceleration of the bimolecular cycloaddition[31] and allows the temperature of reaction to be lowered to 80 °C. Under these conditions the desired cycloadduct **7d** could be isolated in 65% yield. Subsequent DDQ oxidation of **7d** leads to tweezer **2d** in 40% yield. Final dealkylation of the methyl phosphonate **7d** is mildly effected with LiBr[32,33] and affords the desired naphthalene tweezer as lithium salt **2a** in 75% yield. **2a** is soluble in water and methanol

(13) Blokzijl, W.; Engberts, J. B. F. N. *Angew. Chem., Int. Ed.* **1993**, *32*, 1545−1579.
(14) Ferguson, S. B.; Sanford, E. M.; Seward, E. M.; Diederich, F. *J. Am. Chem. Soc.* **1991**, *113*, 5410−5419.
(15) Smithrud, D. B.; Wyman, T. B.; Diederich, F. *J. Am. Chem. Soc.* **1991**, *113*, 5420−5426.
(16) Diederich, F.; Smithrud, D. B.; Sanford, E. M.; Wyman, T. B.; Ferguson, S. B.; Carcanague, D. R.; Chao, I.; Houk, K. N. *Acta Chem. Scand.* **1992**, *46*, 205−215.
(17) Ferguson, S. B.; Seward, E. M.; Diederich, F.; Sanford, E. M.; Chou, P.; Inocencio-Szweda, P.; Knobler, C. B. *J. Org. Chem.* **1988**, *53*, 5593−5595.
(18) Perutz, M. F.; Fermi, G.; Luisi, B. *Acc. Chem. Res.* **1987**, *20*, 309−321.
(19) Hof, F.; Craig, L.; Nuckolls, C.; Rebek, J. J. *Angew. Chem.* **2002**, *114*, 1556−1578.
(20) Rebek, J. J. *Acc. Chem. Res.* **1999**, *32*, 278−286.
(21) Rivera, J. M.; Martin, T.; Rebek, J. J. *J. Am. Chem. Soc.* **1998**, *120*, 819−820.
(22) Vriezema, D. M.; Aragones, M. C.; Elemans, J. A. A. W.; Cornelissen, J. J. L. M.; Rowan, A. E.; Nolte, R. J. M. *Chem. Rev.* **2005**, *105*, 1445−1489.
(23) Witt, D.; Lagona, J.; Damkaci, F.; Fettinger, J. C.; Isaacs, L. *Org. Lett.* **2000**, *6*, 755−758.
(24) Isaacs, L.; Witt, D.; Lagona, J. *Org. Lett.* **2001**, *3*, 3221−3224.
(25) Isaacs, L.; Witt, D. *Angew. Chem.* **2002**, *47*, 1905−1907.
(26) Fokkens, M.; Schrader, T.; Klärner, F. G. *J. Am. Chem. Soc.* **2005**, *127*, 14415−14421.
(27) Jasper, C.; Schrader, T.; Panitzky, J.; Klärner, F.-G. *Angew. Chem., Int. Ed.* **2002**, *41*, 1355−1358.
(28) Fokkens, M.; Jasper, C.; Schrader, T.; Koziol, F.; Ochsenfeld, C.; Polkowska, J.; Lobert, M.; Kahlert, B.; Klärner, F. G. *Chem. Eur. J.* **2005**, *11*, 477−494.
(29) Klärner, F. G.; Kahlert, B.; Boese, R.; Bläser, D.; Juris, A.; Marchioni, F. *Chem.−Eur. J.* **2005**, *11*, 3363−3374.
(30) Benkhoff, J.; Boese, R.; Klärner, F.-G. *Liebigs Ann.-Recl.* **1997**, 501−516.
(31) van Eldik, R.; Klärner, F. G. *High-Pressure Chemistry − Synthetic, Mechanistic, and Supercritical Applications*; Wiley-VCH: Weinheim, 2002.
(32) Rensing, S.; Arendt, M.; Springer, A.; Grawe, T.; Schrader, T. *J. Org. Chem.* **2001**, *66*, 5814−5821.
(33) Krawczyk, H. *Synth. Comm.* **1997**, *27*, 3151−3161.

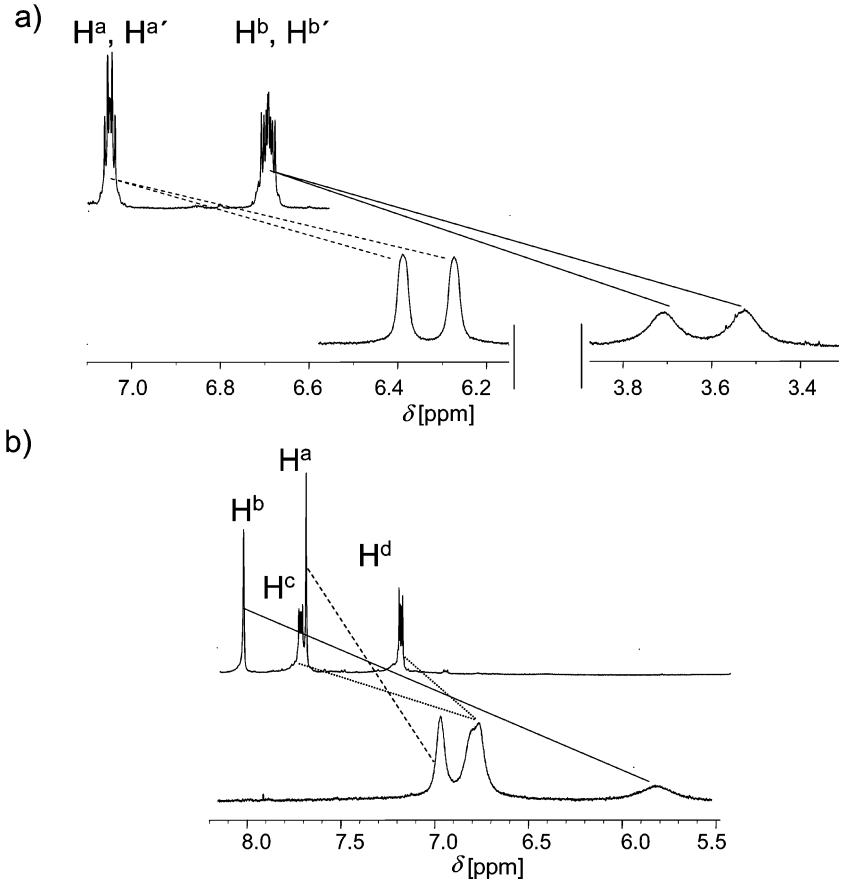

Figure 2. ^{1}H NMR spectra (500 MHz) of (a) **2a** and (b) **4a** in CD_3OD (on top) and D_2O (on bottom).

Table 1. Comparison of the ^{1}H NMR Shifts, δ [ppm], of Tweezer **2a** and Clip **4a** Measured in CD_3OD and D_2O with Those of the Monomeric and Dimeric Structures **2a**, **4a** and $[\mathbf{2a}]_2$, $[\mathbf{4a}]_2$, Respectively, Calculated by the Quantum Chemical Method (GIAO-HF/TZP)[a,b]

receptor	proton	δ_{exp} [CD_3OD]	δ_{calc} monomer	δ_{exp} [D_2O]	δ_{calc} dimer	$\Delta\delta_{exp}$	$\Delta\delta_{calc}$
2a	H^a	7.1 (m)	7.4	6.3 (bs)	6.5, 6.8, δ_{av}: 6.7	0.8	0.7
	$H^{a'}$		7.5	6.4 (bs)	6.7, 7.0, δ_{av}: 6.9	0.7	0.6
	H^b	6.7 (m)	7.0	3.6 (bs)	3.3, 3.5, δ_{av}: 3.4	3.1	3.6
	$H^{b'}$		7.2	3.7 (bs)	4.1, 4.4, δ_{av}: 4.3	3.0	2.9
4a	H^a	7.7 (s)	7.8−8.0	6.9 (bs)	6.0, 6.9, 7.0, 7.4, δ_{av}: 6.8	0.8	1.0−1.2
	H^b	8.1 (s)	8.3	5.8 (bs)	2.6, 4.5, 6.0, 6.6, δ_{av}: 4.9	2.3	3.4
	H^c	7.8 (m)	7.9	6.8 (bm)	6.1, 6.8, 7.1, 7.4, δ_{av}: 6.9	1.0	1.0
	H^d	7.2 (m)	6.9	6.8 (bm)	6.3, 6.4, 6.4, 7.0, δ_{av}: 6.5	0.4	0.4

[a] The geometries for the quantum chemical calculations were optimized by Monte Carlo conformer searches (MacroModel 6.5, Amber*/H_2O).[34] [b] s = singlet; m = multiplet; bs = broad singlet; bm = broad multiplet. δ_{av}: average of δ_{calc}.

as well as comparable to clip **4a**. Detailed procedures of the syntheses of **2a** and **4a** can be found in the Experimental Section.

The structures of all new compounds were characterized by their spectral data (^{1}H NMR, ^{13}C NMR, ^{31}P NMR, IR, and MS). The ^{1}H NMR spectra of **2a** and **4a**, respectively, are surprisingly different in CD_3OD and D_2O and provide experimental evidence for a self-association of both compounds in aqueous solution. By changing the solvent from CD_3OD to D_2O the ^{1}H NMR signals assigned to the protons of the terminal benzene rings H^a, $H^{a'}$ and H^b, $H^{b'}$ of **2a** (Figure 2a) are split from two into four signals and substantially shifted upfield by 0.7 and 3.1 ppm, respectively (Table 1). The resonance frequencies of the signals assigned to the other protons of **2a** are less influenced by the solvent change (Supporting Information: Tables S1−S4). Similar dramatic solvent-dependent upfield shifts of the signals assigned to the anthracene protons are observed in the ^{1}H NMR spectrum of **4a** on transition from methanol to water (Table 1, Figure 2b, Supporting Information: Tables S5−S9). In this case particularly the signal assigned to the protons H^b at the central benzene ring of the anthracene unit is strongest shifted upfield by 2.3 ppm.

The ^{1}H NMR spectra of **2a** and **4a** in CD_3OD solution are not concentration-dependent within the limits of ^{1}H NMR detection ([**2a**] = 8.3−0.05 mM and [**4a**] = 1.5−0.03 mM), indicating that in methanol solution both (tweezer **2a** and clip **4a)** exist as monomers with no detectable tendency to associate. From the large upfield shifts observed for the signals of protons H^b, $H^{b'}$ of **2a** and H^b of **4a** in D_2O we conclude that in each system a distinct structure of self-assembled molecules is formed in which these protons are strongly influenced by the magnetic anisotropy of the arene moieties of neighbor molecules. Geometry optimization of monomeric **2a**, **4a** and dimeric $[\mathbf{2a}]_2$, $[\mathbf{4a}]_2$ by a Monte Carlo conformer search (MacroModel 6.5,

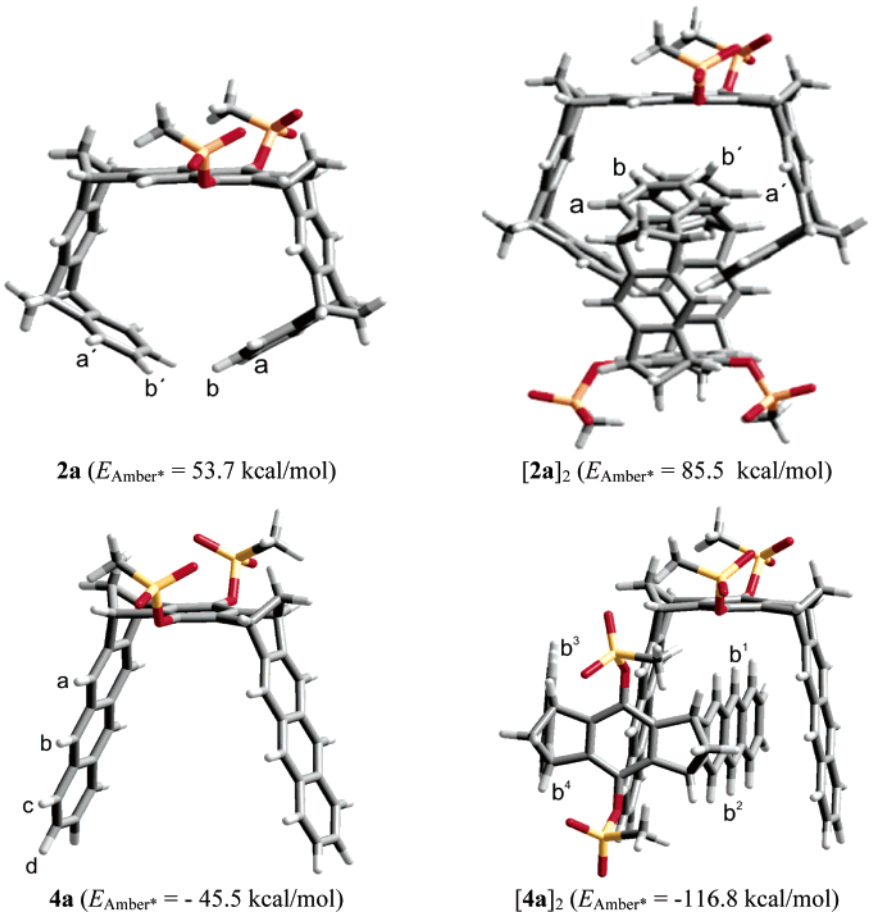

2a (E_{Amber*} = 53.7 kcal/mol) [**2a**]$_2$ (E_{Amber*} = 85.5 kcal/mol)

4a (E_{Amber*} = - 45.5 kcal/mol) [**4a**]$_2$ (E_{Amber*} = -116.8 kcal/mol)

Figure 3. Structures of the monomers **2a** and **4a** and the dimers [**2a**]$_2$ and [**4a**]$_2$ calculated by force field (MacroModel 6.5, Amber*/H_2O, Monte Carlo conformer search, 5000 structures). The structures of dimer [**2a**]$_2$ and [**4a**]$_2$ are chiral; only one enantiomer of each dimer is depicted here. Each dimerization leads to a racemic mixture.

AMBER*/H_2O)[34] led to the low-energy conformers shown in Figure 3.[35] In particular, the large upfield shifts observed for the ^{1}H NMR signals of protons H^b, $H^{b'}$ of **2a** and H^b of **4a** are well explained by the calculated dimer structures. As it will be discussed, the following qualitative structural assignment was later proven by quantum chemical ^{1}H NMR shift calculation (vide infra). In structure [**2a**]$_2$ the protons H^b, $H^{b'}$ of one tweezer molecule are positioned inside the cavity and point toward the central naphthalene spacer unit of the other tweezer molecule and cause the strong magnetic shielding of H^b, $H^{b'}$. In structure [**4a**]$_2$ all four H^b protons are no longer chemically equivalent: one (H^{b1}) of the two protons (which are positioned inside the cavity of the second clip molecule) points toward and the other one (H^{b2}) away from the central benzene spacer unit of the second clip molecule. The other two protons (H^{b3} and H^{b4}) are located outside the cavity with different orientation relative to the central spacer unit of the second clip molecule. Therefore, in the ^{1}H NMR spectrum of [**4a**]$_2$ four signals are expected for the H^b protons, but only the one pointing toward the central spacer unit of the second clip molecule (H^{b1}) is expected to experience substantial shielding. In the spectrum of **4a** in D_2O (Figure 2b) only one signal is observed for these H^b protons, but its specific broadening indicates that a fast exchange between at least two signals takes place leading to an averaged signal. Since the ^{1}H NMR spectra of both compounds **2a** and **4a** in D_2O at room temperature are almost concentration-independent, the observed peak broadening clearly originates from a fast dissociation/association process [**2a**]$_2$ ⇆ 2 **2a** or [**4a**]$_2$ ⇆ 2 **4a** with each equilibrium lying far on the dimer side. Accordingly, at room temperature each equilibration proceeds at a rate comparable to the NMR time scale (Figure 2).

We tried to gain further information on the dimer structures with a mass spectroscopic investigation.[36] The ESI mass spectra recorded in the negative ion mode (electrospray ionization from aqueous and methanol solutions of **2a**) display the peaks of the singly charged dimer [(**2**-(OP(CH$_3$)O$_2^-$)$_2$Li$^+$)$_2$Li$^+$]$^-$ at m/z = 1561.4952 and the singly charged monomer [**2**-(OP(CH$_3$)O$_2^-$)$_2$ Li$^+$]$^-$ at m/z = 777.2317 besides the corresponding monomer and dimer peaks with Na^+ or K^+ as counterions in both solvents. The observation of dimers in the ESI mass spectra supports dimer formation in solution, although they might at least in part be formed as unspecific aggregates.

An unambiguous structural proof of the intertwined dimers [**2a**]$_2$ and [**4a**]$_2$ came from quantum chemical ^{1}H NMR shift

(34) MacroModel 7.1; Schrödinger, Inc.: Portland, OR, 2001.
(35) The ^{1}H NMR data calculated with quantum chemical methods for the conformers of **2a** and **4a** shown in Figure 3 agree best with the experimental data measured in CD_3OD (vide infra). These structures are calculated at the force-field level to be slightly higher in energy by less than 1 kcal/mol in both cases than the energy of the minimum structures of **2a** and **4a** in which both methanephosphonate groups point toward the tweezer or clip cavity (Figures S1, S3).

(36) The MS analysis of this system was performed similarly to that of the host−guest complexes of tweezer **2** (R = OAc) and various bipyridinium salts. Schalley, C. A.; Verhaelen, C.; Klärner, F.-G.; Hahn, U.; Vögtle, F. *Angew. Chem., Int. Ed.* **2005**, *44*, 2477−2480.

calculations. We used structures optimized by force field (AMBER*/H_2O) structures, which we have shown elsewhere[28] to be sufficiently accurate for the computation of chemical shifts. For the systems already described[28] the difference in predicted chemical shifts between AMBER*/H_2O structures and geometries optimized by HF/6-31G** (including distance constraints) was found to be less than 0.4 ppm. Using the AMBER*/H_2O structures of the monomers **2a**, **4a** and the dimers $[\mathbf{2a}]_2$, $[\mathbf{4a}]_2$ chemical shifts were computed by using gauge-including atomic orbitals (GIAO-HF) with SVP and TZP basis sets relative to the TMS reference computed at the same level of theory. Basis-set influences determined by the comparison of the SVP and TZP results are calculated to be small ($\leq$0.3 ppm). All calculations were carried out by using our linear-scaling code[37] as implemented in the program package Q-Chem.[38] In this paper we only compare the strongest solvent-dependent experimental data with the ^{1}H NMR chemical shifts computed at the GIAO-HF/TZP level (Table 1). The detailed comparison of all ^{1}H NMR chemical shift data can be found in the Supporting Information (Tables S1−S9). In the dimer structure $[\mathbf{4a}]_2$ the proton H^{b1} (that points toward the central benzene spacer unit of the second clip molecule) is calculated to be, indeed, dramatically shielded, whereas the protons H^{b2}−H^{b4} (which are positioned away from the central spacer unit or outside of the clip cavity) are calculated to be less shielded. Since in the experimental spectra of tweezer **2a** and clip **4a** in D_2O the observed peak broadening indicates a fast exchange of the protons which are nonequivalent in the dimers but equivalent in the monomers, the comparison of the experimental data with the average of the chemical shifts calculated for one kind of protons (in the monomer) is more reasonable. The ^{1}H NMR chemical shifts calculated for the monomeric tweezer **2a** and clip **4a** are well in accord with the experimental data observed in the corresponding CD_3OD spectra, whereas the shifts calculated for the dimers $[\mathbf{2a}]_2$ and $[\mathbf{4a}]_2$ agree well with those observed in the D_2O spectra. Therefore the comparison of the quantum chemical and experimental results provides strong evidence for the dimerization of tweezer **2a** and clip **4a** in H_2O leading to the structures of $[\mathbf{2a}]_2$ and $[\mathbf{4a}]_2$ shown in Figure 3.

In aqueous solution at room temperature the ^{1}H NMR chemical shifts of $[\mathbf{2a}]_2$ or $[\mathbf{4a}]_2$ are not significantly dependent on the tweezer or clip concentration. In the solution of **2a** dissolved in a CD_3OD/D_2O mixture, they are, however, dependent on the CD_3OD/D_2O ratio indicating a shift of the equilibrium toward the monomer with increasing amount of CD_3OD (for example: $[\mathbf{2a}] = 1.38$ mM: $\delta(H^b$ or $H^{b'})$ in ppm = 3.61 (D_2O), 3.64 (CD_3OD/D_2O = 5:95), 5.92 (CD_3OD/D_2O = 23:77), 6.69 (CD_3OD/D_2O = 50:50), and 6.79 (CD_3OD)). At higher temperatures the concentration dependence of the ^{1}H NMR chemical shifts of tweezer **2a** or clip **4a** in aqueous solution allowed us to determine the equilibrium constants $K_{dim} = [\mathbf{2a}]_2/[\mathbf{2a}]^2$ or $[\mathbf{4a}]_2/[\mathbf{4a}]^2$ of dimerization and the maximum chemical shift differences $\Delta\delta_{max} = \delta$(monomer) − δ(dimer) with the assumption of δ(monomer) being equal to $\delta(CD_3OD)$ (Table 2). In both systems a linear relationship between the values of ln K_{dim} and T^{-1} is observed indicating that for both equilibria the change in the heat capacity is equal to zero ($\Delta C_p = 0$) and the thermodynamic parameters ΔG, ΔH, ΔS can be simply derived from the van't Hoff plots (Figure 4, Table 2).[15,39]

Table 2. Temperature Dependence of the Association Constants, K_{dim} [10^3 M^{-1}], and the Maximum ^{1}H NMR Shifts, $\Delta\delta_{max}$ [ppm], Determined for the Self-Assembling of Tweezer **2a** or Clip **4a** in Aqueous Solution, by ^{1}H NMR Dilution Titration Experiments[a]

	$2 \cdot \mathbf{2a} \rightleftarrows [\mathbf{2a}]_2$			$2 \cdot \mathbf{4a} \rightleftarrows [\mathbf{4a}]_2$		
	T [K]	K_{dim} [10^3 M^{-1}]	$\Delta\delta_{max}$ (H^a or $H^{a'}$)	T [K]	K_{dim} [10^3 M^{-1}]	$\Delta\delta_{max}$ (H^b)
	338	38.2 ± 4.1	0.89	323	27.0 ± 2.5	2.45
	348	16.0 ± 1.6	0.90	338	9.8 ± 1.0	2.46
	358	7.2 ± 0.7	0.91	353	4.2 ± 0.4	2.44
	368	3.2 ± 0.3	0.92	368	2.0 ± 0.2	2.34
ΔH		−20.9 ± 1.5			−13.8 ± 0.9	
$T\Delta S^b$		−12.2 ± 1.2			−6.7 ± 0.8	
ΔG^b		−8.7 ± 1.9			−7.1 ± 1.7	
$K_{dim}{}^b$ [10^5 M^{-1}]		22.8			1.6	

[a] The thermodynamic parameters ΔG [kcal mol^{-1}], ΔH [kcal mol^{-1}], and $T\Delta S$ [kcal mol^-] were calculated from the linear relationship between ln K_{dim} and $1/T$ by using the van't Hoff equation. [b] Values calculated for 298 K by linear regression of the van't Hoff plots (Figure 4).

Table 3. Binding of **8** with Tweezer **2a** and Clip **4a**, **3a** Respectively, in CD_3OD at 298 K

	$\Delta\delta_{max}$ (**8**) [ppm]						
complex	2-H	4-H	5-H	6-H	N–CH_3	K_a [10^4 M^{-1}]	ΔG [kcal mol^{-1}]
8·2a	3.16	1.52	4.80	2.13	2.75	11.9 ± 1.2	−6.93 ± 0.05
8·4a	1.74	2.22	2.38	1.58	1.61	1.04 ± 0.14	−5.48 ± 0.08
8·3a[a]	1.59	3.16	2.98	1.59	1.27	0.17 ± 0.01	−4.39 ± 0.03

[a] See ref 40.

The new tweezer **2a** and clip **4a** form highly stable host−guest complexes with the enzyme cofactor model *N*-methylnicotinamide iodide **8** in methanol. The binding constants, K_a, and the complexation-induced shifts, $\Delta\delta_{max}$, of the guest ^{1}H NMR signals were determined by NMR dilution titrations (Table 3).

The comparison of the binding constants shows that the complexes of the tweezer **8·2a** and the anthracene clip **8·4a** are substantially more stable than that of the naphthalene clip **8·3a**.[40] Evidently, an increase in the number of aromatic binding sites (in tweezer **2a**) and in the van der Waals contact surface (in clip **4a**), respectively, leads to an increase in the complex stability compared to the naphthalene clip **3a.** The large $\Delta\delta_{max}$ values found for the guest protons indicate that the *N*-methylnicotinamide cation is positioned inside the tweezer or clip cavity.

The finding of particularly large $\Delta\delta_{max}$ values for the guest protons 2-H (3.16 ppm) and 5-H (4.80 ppm) of **8·2a** is in full accord with the calculated complex structure (Figure 5). In this structure the guest protons 2-H and 5-H pointing toward the tweezer sidewalls are expected to be stronger influenced by the magnetic anisotropy of the tweezer arene units than those of the guest protons 4-H and 6-H pointing out of the tweezer cavity.[41]

The fact that the $\Delta\delta_{max}$ values of the guest protons observed for complex **8·4a** are of comparable size to those observed for **8·3a** suggests similar geometries for both complexes. The

(37) Ochsenfeld, C.; Kussmann, J.; Koziol, F. *Angew. Chem., Int. Ed.* **2004**, *43*, 4485−4489.
(38) Kong, J.; et al. *J. Comput. Chem.* **2000**, *21*, 1532−1548.
(39) In several host−guest complexations, e.g., between cyclophane hosts and 1,4-disubstituted benzene guests, negative values for ΔC_p are observed. See ref 15.
(40) Polkowska, J.; Klärner, F.-G., unpublished results.

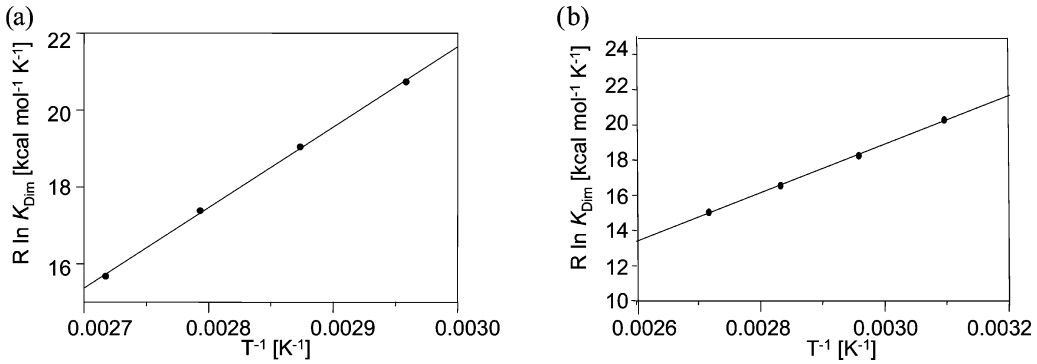

Figure 4. Van't Hoff plots for the self-association of (a) **2a** and (b) **4a** in D_2O.

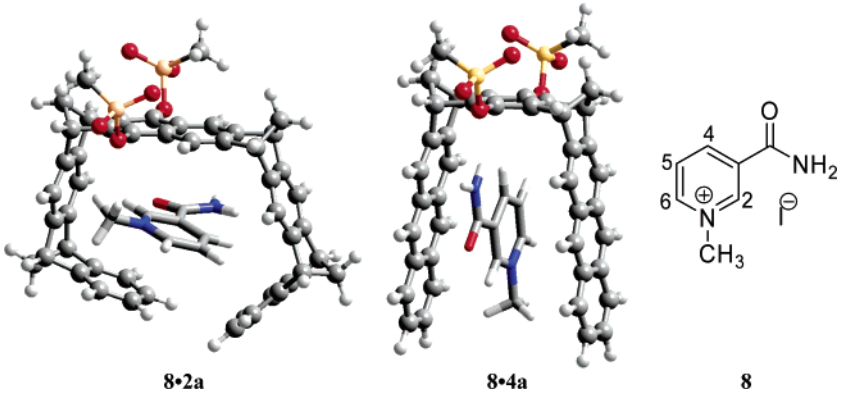

8•2a **8•4a** **8**

Figure 5. Structures of the complexes **8·2a** and **8·4a** calculated by force field (Macro-Model 6.5, Amber*/H_2O, Monte-Carlo conformer search, 5000 structures).

structure calculated for complex **8·4a** (Figure 5) is very similar to that of complex **8·3a** derived from quantum chemical ^{1}H NMR shift calculations.[28] In aqueous solution at room temperature the ^{1}H NMR signals assigned to the protons H^a,$H^{a'}$/H^b,$H^{b'}$ of tweezer **2a** and H^a,H^b,H^c of clip **4a** are shifted downfield from δ [ppm] = 6.3, 6.4/3.6, 3.7 and 6.9, 5.8, 6.8, respectively, to δ [ppm] = 7.0/6.3 and 7.5, 7.7, 7.6, respectively, after addition of equimolar amounts of NMNA **8**. The guest ^{1}H NMR signals of **8** are, however, broad at room temperature so that they cannot be unambiguously assigned. These observations already indicate a shift of the equilibrium $[\mathbf{2a}]_2 \leftrightarrows 2\ \mathbf{2a}$ or $[\mathbf{4a}]_2 \leftrightarrows 2\ \mathbf{4a}$ toward the side of monomeric species resulting from the complex formation **8·2a** or **8·4a** and a dynamic exchange process between complexed and free **8** leading to the specific broadening of the guest ^{1}H NMR signals. Therefore, high-temperature ^{1}H NMR measurements were necessary in order to analyze the undisturbed binding of NMNA **8** by monomeric tweezer **2a** and clip **4a** in aqueous solution. At temperatures between 45 and 95 °C the guest ^{1}H NMR signals of **8** are sufficiently sharp so that they could be assigned and used for NMR dilution titrations. The apparent binding constants, K_a, and the maximum complexation-induced shifts, $\Delta\delta_{max}$, of the guest signals resulting from these measurements are given in Table 4.

Table 4. Temperature Dependence of the Apparent Binding Constants K_a and the Maximum ^{1}H NMR Shifts, $\Delta\delta_{max}$, Induced by the Complex Formation of **8** with Tweezer **2a** or Clip **4a** in Aqueous Solution, Determined by ^{1}H NMR Dilution Titration Experiments[a]

	$[\mathbf{2a}]_{app} + \mathbf{8} \leftrightarrows \mathbf{8{\cdot}2a}$ $[\mathbf{2a}]_{app} = {}^1/_2\,[\mathbf{2a}]_2$			$[\mathbf{4a}]_{app} + \mathbf{8} \leftrightarrows \mathbf{8{\cdot}4a}$ $[\mathbf{4a}]_{app} = {}^1/_2\,[\mathbf{4a}]_2$		
	T [K]	K_a [10^3 M^{-1}]	$\Delta\delta_{max}$ [ppm] (N–CH$_3$)	T [K]	K_a [10^3 M^{-1}]	$\Delta\delta_{max}$ [ppm] (N–CH$_3$)
	338	23.0 ± 2.3	1.4	318	35.0 ± 6.7	1.39
	348	17.7 ± 1.8	1.4	338	17.0 ± 4.6	1.36
	358	13.4 ± 1.3	1.4	358	8.2 ± 1.1	1.34
	368	10.2 ± 1.2	1.5	368	6.0 ± 1.0	1.28
ΔH		−6.7 ± 0.9			−8.2 ± 0.6	
$T\Delta S^b$		0.0 ± 0.0			−1.5 ± 0.2	
ΔG^b		−6.7 ± 1.0			−6.7 ± 1.1	
$K_a{}^b$ [10^3 M^{-1}]		89.4			85.0	

[a] The thermodynamic parameters ΔG [kcal mol^{-1}], ΔH [kcal mol^{-1}], and $T\Delta S$ [kcal mol^{-1}] were calculated from the linear relationship between ln K_a and $1/T$ by using the van't Hoff equation. [b] Values of K_a at 298 K were calculated by linear regression of the van't Hoff plots (Figure 6).

The thermodynamic parameters, the enthalpy, ΔH, entropy, ΔS, Gibbs enthalpy, ΔG, and the apparent binding constant, K_a at 298 K, were determined from the temperature dependence of K_a (Table 4) by the use of the linear van't Hoff plots (Figure 6).

The apparent binding constants for the formation of the complexes **8·2a** and **8·4a** in aqueous solution (K_a = 89 400 or 85 000 M^{-1} at 298 K) starting from the dimeric structures $[\mathbf{2a}]_2$ and $[\mathbf{4a}]_2$ were found to be of equal size and similar to that of the naphthalene clip complex **8·3a** (K_a = 82800 M^{-1})[42] and, in the case of **8·2a**, even smaller than that determined in methanol solution (Table 3). At first glance these findings are surprising

(41) The $\Delta\delta_{max}$ values observed here are of similar size as those found for the protons of *p*-dicyanobenzene and 1,2,3,4-tetracyanobenzene in the complexes with the naphthalene tweezers **2** (R = H, OAc). In these cases the complex structures were determined by X-ray diffraction analysis and quantum chemical ^{1}H NMR shift calculations. Klärner, F.-G.; Burkert, U.; Kamieth, M.; Boese, R.; Benet-Buchholz, J. *Chem.—Eur. J.* **1999**, *5*, 1700−1707. Klärner, F.-G.; Burkert, U.; Kamieth, M.; Boese, R. *J. Phys. Org. Chem.* **2000**, *13*, 1604−1611. Brown, S. P.; Schaller, T.; Seelbach, U. P.; Koziol, F.; Ochsenfeld, C.; Klärner, F.-G.; Spiess, H. W. *Angew. Chem., Int. Ed.* **2001**, *40*, 1717−1720. Ochsenfeld, C.; Koziol, F.; Brown, S. P.; Schaller, T.; Seelbach, U. P.; Klärner, F.-G. *Solid State Nucl. Magn. Reson.* **2002**, *22*, 1128−1153.

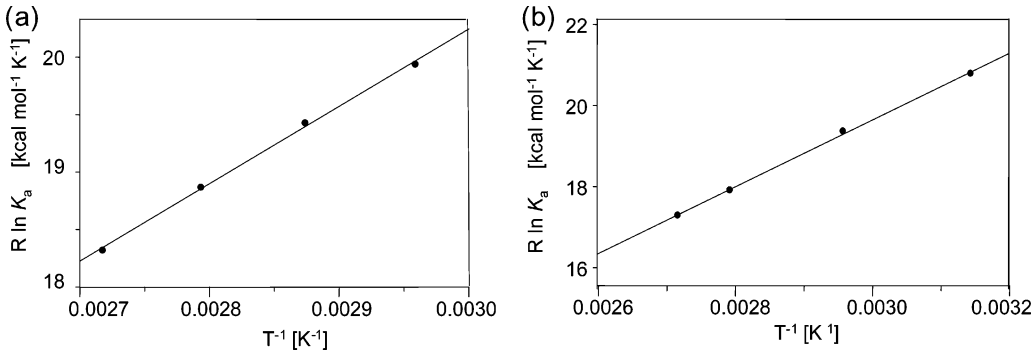

Figure 6. Van't Hoff plots for the complex formation of **8** with (a) **2a** and (b) **4a** in D_2O.

and not consistent with the much higher expectations resulting from literature data.[28,43] This "contradiction", however, can be easily explained if one takes into account that in the complexes **8·2a** and **8·4a** in aqueous solution K_a does not describe the usual equilibrium between the host−guest (1:1) complex and the free guest and the free monomeric host, but in these cases the equilibrium exists among the complex, the guest, and the dimeric host. From the thermodynamic data found for the self-assembly $[\mathbf{2a}]_2 \leftrightarrows 2\ \mathbf{2a}$ or $[\mathbf{4a}]_2 \leftrightarrows 2\ \mathbf{4a}$ and the complex formation $[\mathbf{2a}]_{app} + \mathbf{8} \leftrightarrows \mathbf{8{\cdot}2a}$ or $[\mathbf{4a}]_{app} + \mathbf{8} \leftrightarrows \mathbf{8{\cdot}4a}$ with $[\mathbf{2a}]_{app} = {}^1/_2[\mathbf{2a}]_2$ or $[\mathbf{4a}]_{app} = {}^1/_2[4\mathbf{a}]_2$ we can calculate the true binding constant to be $K_a' = [H{\cdot}G]/([H]{\cdot}[G]) = K_a \cdot K_{dim}{}^{1/2} = 1.3 \times 10^8$ and $3.4 \times 10^7\ M^{-1}$ for the formation of complex **8·2a** and **8·4a**, respectively, starting from the monomeric host and guest molecule.[44] These values impressively show the enormously strong binding of NMNA **8** to tweezer **2a** and clip **4a** in water. They are substantially higher than those found in methanol and also much higher than the K_a value found for formation of complex **8·3a** in aqueous solution.

Conclusion

The profound solvent dependence found for the efficient dimerization of tweezer **2a** and clip **4a** and their strong binding of *N*-methylnicotinamide **8** allows the conclusion that both events are largely the result of a hydrophobic effect. The self-assembly of both compounds as well as their inclusion of **8** are strongly enthalpy driven ($\Delta H \ll 0$, compare Tables 2 and 4). The enthalpic driving force is partially compensated by an unfavorable entropy loss ($T\Delta S < 0$). Similar results of negative enthalpies and entropies of association were also observed for several host−guest complexations in chemical and biological systems in aqueous solution. Molecular recognition of aromatic guest molecules by synthetic cyclophane,[16,17,45,46] hemicarcerand hosts,[47] or in the arene binding pocket at the active site of the digestive serine protease α-chymotrypsine[48] are prominent and typical examples. All these findings are, however, in sharp contrast to a classical hydrophobic effect[13,49,50] (a large favorable positive association entropy, a small favorable enthalpy, and a negative ΔC_p term) but they agree well with the so-called nonclassical hydrophobic effect.[3,16,17] The comparison of the thermodynamic data determined for self-assembly of **2a** and **4a** and their complex formation with NMNA **8** indicate that in the π-cation interaction the enthalpic driving force (resulting from the nonclassic hydrophobic effect) remains while the entropy contribution becomes more favorable (compared to the self-assembly). This finding may be explained by the release of the water molecules solvating the free onium ion.[51] The finding that the benzene-spaced tweezer **1a** shows only negligible tendency ($K_{dim} < 100\ M^{-1}$, $\Delta\delta < 0.1$ ppm)[26] and the naphthalene clip **3a**[28] shows no tendency to form dimers in aqueous solution is remarkable. Evidently, the increase in the van der Waals surface of tweezer **2a** or clip **4a** resulting from the replacement of the benzene spacer unit in **1a** by a naphthalene unit and of the naphthalene sidewalls in **3a** by anthracene moieties leads to the formation of the highly stable dimers $[\mathbf{2a}]_2$ and $[\mathbf{4a}]_2$ in aqueous solution. These results are in fairly good agreement with the semiempirical Stauff rule which says that the stability of micelles in water increases with an increasing number of methylene groups in the nonpolar alkyl chain of a micelle-forming surfactant.[52]

Here we observed an unexpected self-assembly of tweezer **2a** and clip **4a** in aqueous solution evidently as the result of a nonclassical hydrophobic effect. Obviously, the enlargement of the tweezer's and clip's π-faces by an additional benzene ring produces a new host species with perfect self-complementarity. Spontaneous self-assembly is further strongly supported by the rigid preoriented design. The highly ordered intertwined structures of the self-assembled dimers $[\mathbf{2a}]_2$ and $[\mathbf{4a}]_2$ were elucidated by quantum chemical ^{1}H NMR shift calculations. Even more remarkable is the fact that π-cation[53−55] interactions with permanently charged guests can successfully compete with the mutual van der Waals attraction of the electron-rich clip walls and lead to exceedingly stable complexes with the cofactor

(42) Schrader, T.; Fokkens, M.; Klärner, F. G.; Polkowska, J.; Bastkowski, F. *J. Org. Chem.* **2005**, *70*, 10227−10237.
(43) Mordasini Denti, T. Z.; van Gunsteren, W. F.; Diederich, F. *J. Am. Chem. Soc.* **1996**, *118*, 6044−6051.
(44) With $[H]_{app} = {}^1/_2[H]_2$ the true binding constant K_a' is $K_a' = K_a \cdot K_{dim}{}^{1/2} = ([H \cdot G]/[H]_2{}^{1/2} \cdot [G])/([H]_2/[H]^2)^{1/2} = [H \cdot G]/[H] \cdot [G]$.
(45) Claessens, C. G.; Stoddart, J. F. *J. Phys. Org. Chem.* **1997**, *10*, 254−272.
(46) Fyfe, M. C. T.; Stoddart, J. F. *Acc. Chem. Res.* **1997**, *30*, 393−401.
(47) Piatnitski, E. L.; Flowers, R. A., II; Deshayes, K. *Chem.−Eur. J.* **2000**, *6*, 999−1006.
(48) Shiao, D. D. F.; Sturtevant, J. M. *Biochemistry* **1969**, *8*, 4910−4917.
(49) Tanford, C. *The Hydrophobic Effect*, 2nd ed.; Wiley: New York, 1980.
(50) Southall, N. T.; Dill, K. A.; Haymet, A. D. J. *J. Phys. Chem. B* **2002**, *106*, 521−533.
(51) We thank one reviewer for a helpful comment concerning the interpretation of the thermodynamic data.
(52) For most surfactants, there exists a simple relation between the critical micelle concentration cmc and the lengths of the paraffin chains: $\log(\text{cmc}) = A - B \cdot n$, where n denotes the number of carbon atoms and A and B are specific constants, depending on the molecular structure of the surface active compounds. Hoffmann, H.; Ulbricht, W. Physikalische Chemie der Tenside. In *Die Tenside*; Kosswig, K., Stache, H., Eds.; Carl Hanser Verlag: München, Wien, 1993; Chapter 1, pp 31−32. Shinoda, K.; Nakagawa, T.; Tamamushi, B.; Isemura, T. Colloidal Surfactants. *Some Physicochemical Properties*; Academic Press: New York, London, 1963; p 1943.
(53) Gallivan, J. P.; Dougherty, D. A. *J. Am. Chem. Soc.* **2000**, *122*, 870−874.
(54) Gallivan, J. P.; Dougherty, D. A. *Proceedings of the National Academy of Sciences of the United States of America* **1999**, *96*, 9459−9464.
(55) Ma, J. C.; Dougherty, D. A. *Chem. Rev.* **1997**, *97*, 1303−1324.

model NMNA **8** in water.[56] The strong binding of **2a** and **4a** to **8** is an encouraging and promising result for a study of the complex formation with NAD^+ and SAM which is planned, particularly, to answer the question if the two new host molecules bind these enzyme cofactors at their active sites selectively. In the future, we will also try to prevent host dimerization by introducing bulky substituents, so that the full free binding energy of 10−11 kcal/mol can be gained on cofactor inclusion. This should render the new tweezers and clips efficient tools for studying biological processes at physiological conditions.

Experimental Section

IR: Bio-Rad FTS 135. UV−vis: Varian Cary 300 Bio. ^{1}H NMR, ^{13}C NMR, ^{31}P NMR, DEPT H, H-COSY, C, H-COSY, NOESY, HMQC, HMBC: Bruker DRX 500. ^{1}H NMR titration experiments: Bruker DRX 500; the undeuterated amount of the solvent was used as an internal reference. In the high-temperature measurements dichloromethane or acetone was used as an internal reference. Positions of the protons of the methylene bridges are indicated by the letters *i* (*innen*, toward the center of the molecule) and *a* (*aussen*, away from the center of the molecule). MS: Bruker BioTOF II (ESI). All melting points are uncorrected. Column chromatography: silica gel 0.063−0.2 mm. All solvents were distilled prior to use.

Dimethyl(1α,4α,7α,10α)1,4,7,10-tetrahydro-1,4:7,10-dimethanonaphthacene-5,12-diyl-bis(methanephosphonate) (5d): Dropwise addition of triethylamine (0.9 mL, 6.72 mmol) to a stirred, cold (0 °C) solution of hydroquinone **5b** (R = OH, 0.75 g, 2.6 mmol) and methanephosphonic acid dichloride (1.44 g, 10.8 mmol) in anhydrous THF (75 mL) under argon led to the immediate precipitation of a colorless solid. After 1 h the mixture was allowed to warm to rt and stirred for another 20 h. The precipitate was dissolved after the addition of 45 mL of methanol. The solution was stirred for 3 h at rt and concentrated in vacuo to the half of its volume. The precipitated ammonium chloride was filtered off, and the filtrate was evaporated in vacuo. The remaining crude product was purified by column chromatography (Florisil, acetone/cyclohexane 1:1). Yield: 370 mg **5d** (0.78 mmol, 30%).

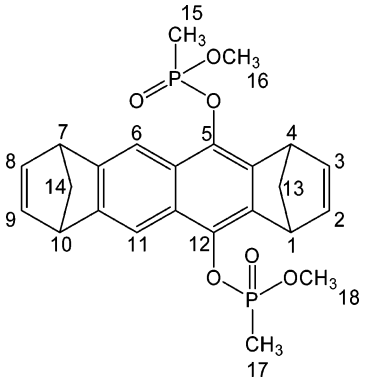

Mp: 163 °C. ^{1}H NMR (500 MHz, $CDCl_3$): δ [ppm] = 1.65 (dm, 6 H, 15-H, 17-H, ^2J (15-H, P and 17-H, P) = 17.5 Hz), 2.25 (m, 4 H, 13-H, 14-H), 3.72 (m, 6 H, 16-H, 18-H), 3.96 (s, 2 H, 7-H, 10-H), 4.37 (m, 2 H, 1-H, 4-H), 6.69 (m, 2 H, 8-H, 9-H), 6.77 (m, 2 H, 2-H, 3-H), 7.73 (m, 2 H, 6-H, 11-H). ^{13}C NMR (125 MHz, $CDCl_3$): δ [ppm] = 11.07 (dm, C-15, C-17, ^1J (C-15, P and C-17, P) = 143.9 Hz), 48.21 (s, C-1, C-4), 49.83 (s, C-7, C-10), 52.96 (m, C-16, C-18), 65.63/65.71/65.79 (3 s; C-13), 67.26 (m, C-14), 113.88 (m, C-2, C-3, C-8, C-9), 125.27 (m, C-5a, C-11a), 136.51 (m, C-6a, C-10a), 138.54 (m, C-4a, C-12a), 142.18 (m, C-6, C-11), 149.64 (C-5, C-12). ^{31}P NMR (200 MHz, $CDCl_3$): δ [ppm] = 30.36 (s, 2 P). MS (ESI, positive ion mode, MeOH): m/z = 473 [M + H^+], 495 [M + Na^+], 511 [M + K^+].

Dimethyl(5α,7α,10α,12α,17α,19α,22α,24α)-5,6,6a,7,10,10a,11,12,-17,18,18a,19,22,22a,23,24-hexadecahydro-5,24:7,22:10,19:12,17-tetramethanodecacene-8,21-diyl-bis(methane-phosphonate) (7d): Bisdienophile **5d** (180 mg, 0.38 mmol), diene **6** (260 mg, 1.54 mmol), and ca. 0.5 mg Bis(3-*tert*-butyl-4-hydroxy-5-methanephenyl)-sulfide (BHMPS) were dissolved in a mixture of anhydrous toluene (2.5 mL) and anhydrous acetonitrile (0.5 mL). After saturation with argon the solution was placed into a PTFE shrinkage tube (deactivated by hot triethylamine and dried in vacuo), and the sealed tube was placed into the preheated (80 °C) autoclave. The solution was heated to 80 °C at a pressure of 12 kbar for 6 h. After the autoclave cooled to rt overnight, the solution was evaporated in vacuo. The residual was dissolved in acetone, the precipitated solid was filtered off, and the clear solution was purified by MPLC (Florisil, cyclohexane/ethyl acetate 1:1). Yield: 200 mg (0.25 mmol, 65%) of the bisadduct **7d** as a colorless solid.

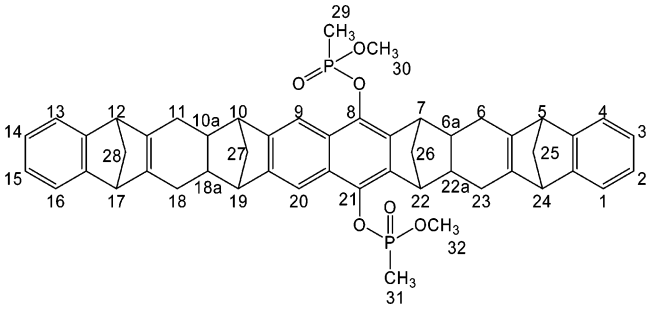

Mp: 167 °C. ^{1}H NMR (500 MHz, $CDCl_3$): δ [ppm] = 1.56 (m, 2 H, 26-H^a, 27-H^a); 1.66 (dm, 6 H, 29-H, 31-H, ^2J (29-H, P and 31-H, P) = 17.5 Hz); 1.71 (m, 4 H, 6a-H, 10a-H, 18a-H, 22a-H); 2.09 (2 H, 26-H^i, 27-H^i); 2.23 (m, 8 H, 6-H, 11-H, 18-H, 23-H); 2.44 (m, 4 H, 25-H, 28-H); 3.11 (s, 2 H, 10-H, 19-H); 3.49 (s, 2H, 7-H, 22-H); 3.60 (m, 4 H, 5-H, 12-H, 17-H, 24-H); 3.70 (dm, 6 H, 30-H, 32-H, ^3J (30-H, P and 32-H, P) = 11.2 Hz); 6.80 (m, 4 H, 2-H, 3-H, 14-H, 15-H); 7.11 (m, 4 H, 1-H, 4-H, 13-H, 16-H); 7.64/7.65 (s, 2H, 9-H, 20-H). ^{13}C NMR (125 MHz, CD_3OD): δ [ppm] = 10.70/11.87 (C-29, C-31), 29.69 (C-6, C-11, C-18, C-23), 39.89 (C-6a, C-22a), 40.67 (C-10a, C-18a), 44.22 (C-26, C-27), 50.56 (C-10, C-19), 52.72 (C-30, C-32), 53.12 (C-7, C-22), 53.81 (C-5, C-12, C-17, C-24), 66.64 (C-25), 69.66 (C-28), 112.53 (C-9, C-20), 120.76 (C-1, C-4, C-13, C-16), 124.04 (C-2, C-3, C-14, C-15), 126.49 (C-8a, C-20a), 135.78 (C-7a, C-21a), 147.39 (C-5a, C-11a, C-17a, C-23a), 148.09 (C-9a, C-19a), 151.78 (C-8, C-21), 152.14 (C-4a, C-12a, C-16a, C-24a). ^{31}P NMR (200 MHz, CD_3OD): δ [ppm] = 28.76/28.85 (s, 2 P). MS (ESI, positive ion mode, MeOH): m/z = 831 [M + Na^+], 1640 [$(M)_2$ + Na^+], 2448 [$(M)_3$ + Na^+]. HRMS (ESI, positive ion mode, MeOH) m/z: calcd for $C_{50}H_{50}O_6P_2Na$, 831.298; found, 831.302.

Dimethyl(5α,7α.10α,12α,17α,19α,22α,24α)-5,7,10,12,17,19,22,24-octahydro-5,24:7,22:10,19:12,17-tetramethanodecacene-8,21-diyl-bis(methanephosphonate) (2d): Under argon **7d** (140 mg, 0.17 mmol) and 2,3-dichloro-5,6-dicyanobenzoquinone (DDQ) (380 mg, 1.67 mmol) were dissolved in 6 mL of dry, hot toluene (110 °C) and stirred 2 h under reflux. After cooling to 40 °C, 1,3-cyclohexadiene (0.15 mL, 126 mg, 1.57 mmol) was added to remove reactive DDQ residuals. The mixture was evaporated in vacuo and dissolved in chloroform, and the insoluble byproduct was filtered off. The filtrate was evaporated to dryness, dissolved in a small amount of acetone, and purified by column chromatography (Florisil, ethyl acetate). Yield: 56 mg (0.068 mmol, 40%) of tweezer **2d**.

(56) Scharer, K.; Morgenthaler, M.; Paulini, R.; Obst-Sander, U.; Banner, D. W.; Schlatter, D.; Benz, J.; Stihle, M.; Diederich, F. *Angew. Chem., Int. Ed.* **2005**, *44*, 4400−4404.

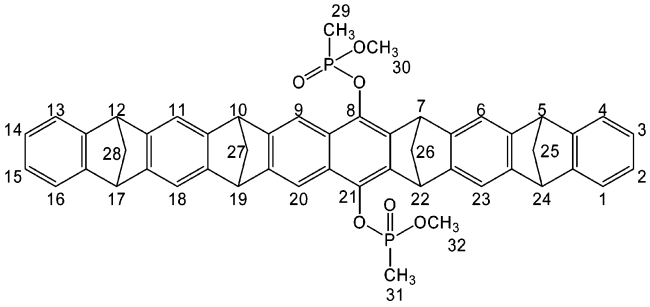

Mp: 182 °C. ^{1}H NMR (500 MHz, CD_3OD): δ [ppm] = 1.59 (dm, 6 H, 29-H, 31-H, ^2J (29-H, P and 31-H, P) = 17.6 Hz); 2.41 (m, 8 H, 25-H, 26-H, 27-H, 28-H); 3.39 (dm, 6 H, 30-H, 32-H, ^3J (30-H, P und 32-H, P) = 11.3 Hz); 4.11 (m, 2 H, 12-H, 17-H); 4.14 (m, 2 H, 5-H, 24-H); (m, 2 H, 10-H, 19-H); 4.62/4.65 (s, 2 H, 7-H, 22-H); 6.68 (m, 4 H, 2-H, 3-H, 14-H. 15-H); 7.05 (m, 4 H, 1-H, 4-H, 13-H, 16-H); 7.21 (m, 2 H, 11-H, 18-H); 7.32/7.35 (m, 2H, 6-H, 23-H); 7.64/7.71 (m, 2 H, 9-H, 20-H). ^{13}C NMR (125 MHz, CD_3OD): δ [ppm] = 9.96/11.11 (d, C-29, C-31), 50.10 (C-10, C-19), 52.37 (C-5, C-24), 52.60 (C-12, C-17), 54.01/54.08 (d, C-30, C-32), 66.73 (s, C-26), 67.71 (s, C-27), 68.73 (s, C-25), 69.09 (s, C-28), 114.75/114.99 (d, C-9, C-20), 117.32/117.44 (d, C-6, C-23), 118.30 (C-11, C-18), 122.41 (s, C-1, C-4, C-13, C-16), 125.82 (s, C-2, C-3, C-14, C-15), 126.98 (s, C-8a, C-20a), 137.85 (s, C-9a, C-19a), 138.84/139.19 (s, C-7a, C-21a), 147.19 (s, C-10a, C-18a), 147.87/147.97 (d, C-6a, C-22a), 149.87 (m, C-5a, C-11a, C-17a, C-23a), 150.77/150.92 (d, C-8, C-21), 152.11 (m, C-4a, C-12a, C-16a, C-24a), chemical shifts for C-7, C-22 were not detected because of overlap with the CD_3OD signal. ^{31}P NMR (200 MHz, CD_3OD): δ [ppm] = 30.92/31.26 (s, 2 P). MS (ESI, positive ion mode, MeOH): m/z = 801 [M + H$^+$], 823 [M + Na$^+$], 1623 [(M)$_2$ + Na$^+$].

Bislithium(5α,7α,10α,12α,17α,19α,22α,24α)-5,7,10,12,17,19,22,-24-octahydro-5,24:7,22:10,19:12,17-tetramethanodecacene-8,21-diyl-(bismethanephosphonate) (2a): Tweezer **2d** (40 mg, 0.051 mmol) and anhydrous lithium bromide (10.6 mg, 0.12 mmol) were dissolved in anhydrous acetonitrile (5 mL) under argon. While the mixture was stirred under reflux for 20 h, the product precipitated as a bright solid. After the mixture was cooled to rt, the solid was filtered off and washed twice with small portions of hot acetonitrile. The product was dried in vacuo. Yield: 30 mg (0.038 mmol, 75%) of the bislithiumphosphonate tweezer **2a** as a colorless solid.

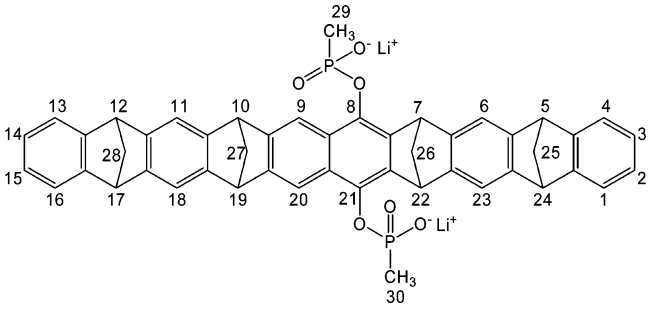

Decomp > 255 °C. ^{1}H NMR (500 MHz, CD_3OD): δ [ppm] = 1.20 (d, 6 H, 29-H, 30-H, ^2J (29-H, P and 30-H, P) = 16.5 Hz), 2.31 (2 H, 26-H), 2.40 (m, 6 H, 25-H, 27-H, 28-H), 4.09 (s, 2 H, 12-H, 17-H), 4.10 (s, 2 H, 5-H, 24-H), 4.21 (s, 2 H, 10-H, 19-H), 4.77 (s, 2 H, 7-H, 22-H), 6.69 (m, 4 H, 2-H, 3-H, 14-H. 15-H), 7.05 (m, 4 H, 1-H, 4-H, 13-H, 16-H), 7.16 (s, 2 H, 11-H, 18-H), 7.35 (s, 2 H, 6-H, 23-H), 7.88 (s, 2 H, 9-H, 20-H). ^{13}C NMR (125 MHz, CD_3OD): δ [ppm] = 13.78 (d, C-29, C-30, ^1J (C-29, P and C-30, P) = 137.8 Hz), 50.03 (s, C-7, C-22), 52.38 (s, C-10, C-19), 52.62 (2 s, C-5, C-12, C-17, C-24), 67.15 (s, C-26), 67.79 (s, C-27), 68.96 (s, C-25, C-28), 116.03 (s, C-9, C-20), 117.21 (s, C-11, C-18), 118.06 (s, C-6, C-23), 122.40 (s, C-1, C-4, C-13, C-16), 125.71 (s, C-2, C-3, C-14, C-15), 128.11 (s, C-8a, C-20a), 138.09 (s, C-9a, C-19a), 139.42 (d, C-7a, C-21a, ^3J (C-7a, P and C-21a, P) = 7 Hz), 148.31 (s, C-6a, C-22a), 148.40 (s, C-10a, C-18a), 148.51 (s, C-11a, C-17a), 149.01 (s, C-5a, C-23a), 149.32 (s, C-8, C-21), 152.14 (s, C-4a, C-24a), 152.27 (s, C-12a, C-16a). ^{31}P NMR (200 MHz, CD_3OD): δ [ppm] = 21.66 (s, 2 P). MS (ESI, negative ion mode, MeOH): m/z = 385 [(M)$_2$], 771 [M + H$^+$], 793 [M + Na$^+$]. HRMS (ESI, negative ion mode, MeOH) m/z: calcd for $C_{48}H_{36}O_6P_2$, 385.100; found, 385.101. UV/vis (H_2O): λ_{max} [nm] (lg ϵ) = 258 (4.640), 294 (4.481). IR (KBr): $\tilde{\nu}$ [cm^{-1}] = 2973 (CH), 2935 (CH), 2862 (CH), 1647 (C═C), 1193 (P═O), 1068 (P—O).

(7α,9α,18α,20α)-7,9,18,20-Tetrahydro-7,20:9,18-dimethanononacene-8,19-diyl-bis(methanephosphonic acid) (4c): Dropwise addition of triethylamine (67 μL, 0.50 mmol) to the stirred solution of the hydroquinone clip **4b** (100 mg, 0.19 mmol) and methanephosphonic acid dichloride (67 mg, 0.50 mmol) in anhydrous THF at 0 °C under argon led to the immediate precipitation of a colorless solid. After 1 h the mixture was allowed to warm to rt and was stirred for another 1 h. The precipitate was filtered off under argon, and 2.5% aqueous HCl (3 mL) was added to the stirred filtrate. After 15 min *n*-hexane (5 mL) was added, and the resulting two-layer system was stirred overnight resulting in the precipitation of a colorless solid. The solid was filtered off, washed with small amounts of 2.5% aqueous HCl, and dried in vacuo over P_2O_5 to furnish 87 mg (0.13 mmol, 67%) of the phosphonic acid clip **4c**.

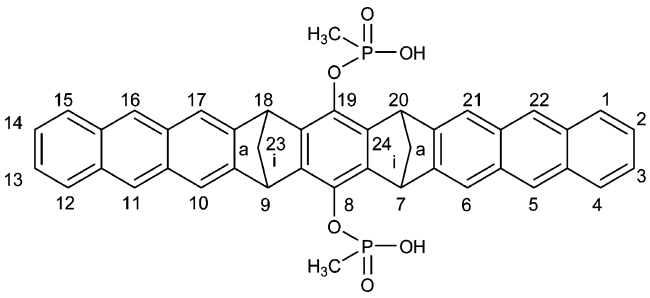

Mp > 300 °C. ^{1}H NMR (500 MHz, DMSO): δ [ppm] = 1.69 (d, 6 H, ^2J(P, —CH$_3$) = 17.2 Hz, —CH$_3$), 2.34 (d, 2 H, ^2J(23i-H, 23a-H) = 8.1 Hz, 23a-H, 24a-H), 2.52 (d, 2 H, 23i-H, 24i-H), 3.34 (s, 2 H, —OH), 4.71 (s, 4 H, 7-H, 9-H, 18-H, 20-H), 7.33 (m, 4 H, 2-H, 3-H, 13-H, 14-H), 7.76 (s, 4 H, 6-H, 10-H, 17-H, 21-H), 7.88 (m, 4 H, 1-H, 4-H, 12-H, 15-H), 8.21 (s, 4 H, 5-H, 11-H, 16-H, 22-H). ^{13}C NMR (125 MHz, DMSO): δ [ppm] = 12.67 (dq, ^1J(P, —CH$_3$) = 140.2 Hz, —CH$_3$), 47.51 (d, C-7, C-9, C-18, C-20), 63.28 (t, C-23, C-24), 119.60 (d, C-6, C-10, C-17, C-21), 124.86 (d, C-2, C-3, C-13, C-14), 125.48 (d, C-5, C-11, C-16, C-22), 127.67 (d, C-1, C-4, C-12, C-15), 130.23 (s, C-5a, C-10a, C-16a, C-21a), 130.87 (s, C-4a, C-11a, C-15a, C-22a), 135.84 (s, C-8, C-19), 140.22 (s, C-7a, C-8a, C-18a, C-19a), 145.37 (s, C-6a, C-9a, C-17a, C-20a). ^{31}P NMR (202.4 MHz, DMSO-d_6): δ [ppm] = 26.60 (s). IR (KBr): $\tilde{\nu}$ [cm^{-1}] = 3428 (OH), 3050 (CH), 3013 (CH), 2968 (CH), 2939 (CH), 2862 (CH), 1465 (C═C), 1312 (P═O), 1181 (P—O). UV/vis (MeOH): λ_{max} [nm] (lg ϵ) = 318 (3.93), 334 (4.06), 351 (4.14), 370 (4.02). MS (ESI, MeOH/DMSO, positive ion mode): m/z = 695 [M + H$^+$], 717 [M + Na$^+$], 773 [M + DMSO + H$^+$], 1389 [(M)$_2$ + H$^+$], 1411 [(M)$_2$ + Na$^+$], 2083 [(M)$_3$ + H$^+$], 2105 [(M)$_3$ + Na$^+$]. HRMS (ESI, positive ion mode, MeOH/DMSO) m/z: calcd for $C_{42}H_{33}O_6P_2$, 695.174; found, 695.175.

Bis(tetra-*n*-butylammonium)(7α,9α,18α,20α)-7,9,18,20-tetrahydro-7,20:9,18-dimethano-nonacene-8,19-diyl-bis(methanephosphonate) (4e): Tetra-*n*-butylammonium hydroxide (144 μL, 1 M solution in methanol) was added to the stirred suspension of **4c** (50 mg, 0.072 mmol) in dichloromethane (50 mL). The mixture was stirred at rt for 2 h, and then the solvent was evaporated in vacuo. In the case the ^{1}H NMR analysis of this crude product indicated a small excess of tetra-*n*-butylammonium hydroxide, the product was again dissolved in methanol, and equivalent amounts of the missing acid **4c** were added

under vigorous stirring. After 1 h of stirring at rt, the solid was filtered off and the filtrate was again dried in vacuo to furnish 85 mg (0.072 mmol, 100%) of the phosphonate clip **4e** as a light brown solid.

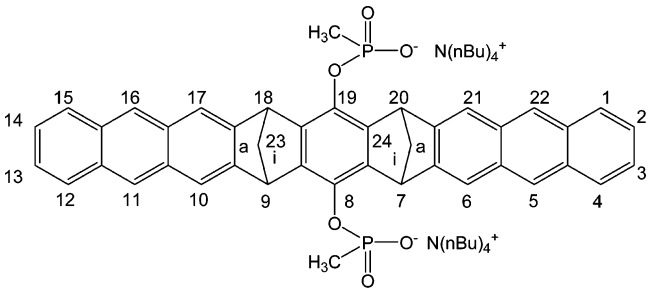

4e

Decomp > 170 °C. ^{1}H NMR (500 MHz, $CDCl_3$): δ [ppm] = 0.76 (t, 24 H, ^2J(γ-H, δ-H) = 6.9 Hz, δ-H), 1.06 (m, 16 H, γ-H), 1.16 (s, 16 H, β-H), 1.59 (d, 6 H, ^2J(P, —CH_3) = 16.6 Hz, —CH_3), 2.30 (d, 2 H, ^2J(23i-H, 23a-H) = 5.4 Hz, 23a-H, 24a-H), 2.64 (d, 2 H, 23i-H, 24i-H), 2.68 (s, 16 H, α-H), 4.94 (s, 4 H, 7-H, 9-H, 18-H, 20-H), 7.14 (m, 4 H, 2-H, 3-H, 13-H, 14-H), 7.58 (m, 4 H, 1-H, 4-H, 12-H, 15-H), 7.63 (s, 4 H, 6-H, 10-H, 17-H, 21-H), 7.80 (s, 4 H, 5-H, 11-H, 16-H, 22-H). ^{13}C NMR (125 MHz, $CDCl_3$): δ [ppm] = 13.40 (dq, ^1J(P, —CH_3) = 135.0 Hz, —CH_3), 13.61 (q, C-δ), 19.42 (t, C-γ), 23.63 (t, C-β), 48.26 (d, C-7, C-9, C-18, C-20), 58.24 (t, C-α), 63.03 (t, C-23, C-24), 119.26 (d, C-6, C-10, C-17, C-21), 124.60 (d, C-2, C-3, C-13, C-14), 125.21 (d, C-5, C-11, C-16, C-22), 127.66 (d, C-1, C-4, C-12, C-15), 130.89 (s, C-4a, C-11a, C-15a, C-22a)*, 131.17 (s, C-5a, C-10a, C-16a, C-21a)*, 137.88 (ds, ^2J(P, C-8) = 3.7 Hz, C-8, C-19), 140.34 (s, C-7a, C-8a, C-18a, C-19a), 147.69 (s, C-6a, C-9a, C-17a, C-20a).^{31}P NMR (202.4 MHz, $CDCl_3$): δ [ppm] = 20.41 (s). IR (KBr): $\tilde{\nu}$ [cm^{-1}] = 3040 (CH), 2963 (CH), 2939 (CH), 2872 (CH), 1467 (C═C), 1291 (P═O), 1183 (P—O). UV/vis (MeOH): λ_{max} [nm] (lg ϵ) = 337 (3.97), 354 (4.07), 373 (3.92). MS (ESI, MeOH, positive ion mode): *m*/*z* = 1419 [M + N(*n*-Bu)$_4^+$], 1200 [M + Na^+], 1178 [M + H^+], 936 [M − N(*n*-Bu)$_4^+$ + 2 H^+], 717 [M − 2 N(*n*-Bu)$_4^+$ + Na + 2 H^+], 242 [N(*n*-Bu)$_4^+$]. HRMS (ESI, positive ion mode, MeOH) *m*/*z*: calcd for $C_{74}H_{103}N_2O_6P_2$, 1177.729; found, 1177.731.

The assignment of the signals of (C-4a, C-11a, C-15a, C-22a) and (C-5a, C-10a, C-16a, C-21a) is not unambiguous and maybe interchanged because the digital resolution of the 2D-NMR spectra (HMBC) is not high enough to separate these signals.

Bislithium(7α,9α,18α,20α)-7,9,18,20-tetrahydro-7,20:9,18-dimethanononacene-8,19-diyl-bis(methanephosphonate) (4a): Lithium-monohydrate hydroxide (0.7 mL, 0.2 M solution in methanol) was added to the stirred suspension of **4c** (50 mg, 0.072 mmol) in dichloromethane (50 mL). The mixture was stirred at rt for 2 h, and then the solid was filtered off. The solvent was removed in vacuo to furnish 45 mg (0.064 mmol, 87%) of the phosphonate clip **4a** as a light brown solid.

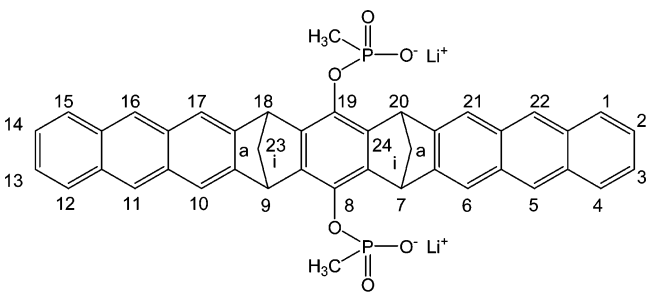

Decomp > 230 °C. ^{1}H NMR (500 MHz, CD_3OD): δ [ppm] = 1.39 (d, 6 H, ^2J(P, —CH_3) = 16.4 Hz, —CH_3), 2.34 (dt, 2 H, ^2J(23i-H, 23a-H) = 8 Hz, ^3J(23a-H, 9-H) = 1.6 Hz, 23a-H, 24a-H), 2.64 (dt, 2 H, ^3J(23i-H, 9-H) = 1.4 Hz, 23i—H, 24i-H), 4.83 (t, 4 H, 7-H, 9-H, 18-H, 20-H), 7.24 (m, 4 H, 2-H, 3-H, 13-H, 14-H), 7.74 (s, 4 H, 6-H, 10-H, 17-H, 21-H), 7.77 (m, 4 H, 1-H, 4-H, 12-H, 15-H), 8.08 (s, 4 H, 5-H, 11-H, 16-H, 22-H). ^{13}C NMR (125 MHz, CD_3OD): δ [ppm] = 13.61 (dq, ^1J(P, —CH_3) = 136.9 Hz, —CH_3), 49.43 (d, C-7, C-9, C-18, C-20), 64.25 (t, C-23, C-24), 120.37 (d, C-6, C-10, C-17, C-21), 125.52 (d, C-2, C-3, C-13, C-14), 126.52 (d, C-5, C-11, C-16, C-22), 128.78 (d, C-1, C-4, C-12, C-15), 132.41 (s, C-5a, C-10a, C-16a, C-21a), 132.78 (s, C-4a, C-11a, C-15a, C-22a), 139.24 (dds, ^2J(P, C-8) = 8.1 Hz, ^5J(P, C-8) = 1.9 Hz, C-8, C-19), 141.60 (s, C-7a, C-8a, C-18a, C-19a), 147.85 (s, C-6a, C-9a, C-17a, C-20a). ^{31}P NMR (202.4 MHz, CD_3OD): δ [ppm] = 21.54 (s); IR (KBr): $\tilde{\nu}$ [cm^{-1}] = 3051 (CH), 2937 (CH), 2862 (CH), 1467 (C═C), 1290 (P═O), 1185 (P—O). UV/vis (MeOH): λ_{max} [nm] (lgϵ) = 318 (3.82), 334 (3.99), 351 (4.08), 370 (3.93). MS (ESI, MeOH, positive ion mode): *m*/*z* = 1419 [M_2 + Li^+], 745 [M − Li^+ + 2 Na^+], 713 [M + Li^+]. MS (ESI, MeOH, negative ion mode): *m*/*z* = 699 [M − Li^+], 346 [M − 2 Li^+]. HRMS (ESI, negative ion mode, MeOH) *m*/*z*: calcd for $C_{42}H_{30}O_6P_2$, 346.076; found, 346.076.

Determination of K_{dim}, ^{1}H NMR Titration Method: Two receptor molecules R are in equilibrium with their dimer RR (2 R ⇆ RR). The self-association constant K_{dim} is defined by eq 1. $[R]_0$ is the total concentration of the receptor.

$$K_{dim} = \frac{[RR]}{[R]^2} = \frac{[RR]}{([R]_0 - 2 \cdot [RR])^2} \quad (1)$$

The observed chemical shift δ_{obs} of the receptor in the ^{1}H NMR spectrum is an averaged value between the monomeric (δ_0) and dimeric structure (δ_{max}) of the receptor, provided that the association/dissociation is fast with respect to the NMR time scale (eq 2). Combination of eqs 1 and 2 and the use of differences in chemical shifts ($\Delta\delta = \delta_0 - \delta_{obs}$; $\Delta\delta_{max} = \delta_0 - \delta_{max}$) lead to eq 3.

$$\delta_{obs} = \frac{[R]}{[R]_0} \cdot \delta_0 + \frac{2 \cdot [RR]}{[R]_0} \cdot \delta_{max} \quad (2)$$

$$\Delta\delta = \frac{\Delta\delta_{max}}{[R]_0} \cdot \left[[R]_0 + \frac{1}{4 \cdot K_{dim}} - \sqrt{\frac{[R]_0}{2 \cdot K_{dim}} + \frac{1}{16 \cdot K_{dim}}} \right] \quad (3)$$

In the titration experiments a defined amount of receptor was dissolved in a defined volume of D_2O. From this reference sample aliquots were taken and diluted with a defined volume of D_2O. Measurement of the averaged chemical shift (δ_{obs}) of the receptor dependent on the concentration afforded the data pairs $\Delta\delta$ and $[R]_0$. Fitting of these data to eq 3 by iterative methods delivered the parameters K_{dim} and $\Delta\delta_{max}$. These parameters were independently determined for each proton of the receptor showing concentration-dependent chemical ^{1}H NMR shifts.

The binding constants, K_a, and the complexation-induced ^{1}H NMR shifts, $\Delta\delta_{max}$, were determined for the host—guest complex formation between tweezer **2a** or clip **4a** as host molecules and NMNA **8** as guest molecule by ^{1}H NMR dilution titration experiments as described in ref 28.

Acknowledgment. We thank Prof. Dr. Christoph Schalley for performing the ESI-MS investigations and Prof. Dr. Heinz Rehage for helpful discussions. This work has been supported by the DFG (Deutsche Forschungsgemeinschaft). C.O. acknowledges financial support by an Emmy Noether research grant of the DFG, and J.Z. financial support by a fellowship of LGFG (Landesgraduiertenfoerderungsgesetz).

Supporting Information Available: Calculation of the tweezer and clip structures **2a**, **[2a]$_2$**, **4a**, **[4a]$_2$** by force-field methods and the chemical ^{1}H NMR shifts by quantum chemical methods;

the experimental data for the determination of the association constants, K_{dim} or K_a, and the complexation-induced ^{1}H NMR shifts, $\Delta\delta_{max}$, by the ^{1}H NMR dilution titration experiments at variable temperature. This material is available free of charge via Internet at http://pubs.acs.org.

JA058410G